Chin. Phys. B Vol. 19, No. 6 (2010) 060506

Generating one-, two-, three- and four-scroll attractors from a novel four-dimensional smooth autonomous chaotic system

Sara Dadras and Hamid Reza Momeni†

Automation and Instruments Lab, Electrical Engineering Department, Tarbiat Modares University, P.O. Box 14115-143, *Tehran, Iran*

(Received 20 October 2009; revised manuscript received 9 December 2009)

A new four-dimensional quadratic smooth autonomous chaotic system is presented in this paper, which can exhibit periodic orbit and chaos under the conditions on the system parameters. Importantly, the system can generate one-, two-, three- and four-scroll chaotic attractors with appropriate choices of parameters. Interestingly, all the attractors are generated only by changing a single parameter. The dynamic analysis approach in the paper involves time series, phase portraits, Poincaré maps, a bifurcation diagram, and Lyapunov exponents, to investigate some basic dynamical behaviours of the proposed four-dimensional system.

Keywords: new smooth autonomous four-dimensional chaotic system, multi-scroll chaotic attractor, Poincaré mapping, bifurcation, Lyapunov exponent

PACC: 0545

1. Introduction

In 1963, Lorenz found the first chaotic attractor.[1] Lorenz's discovery is a third-order autonomous system with only two quadratic nonlinearities but it can display very complex dynamical behaviours. In particular, the Lorenz system can produce the well-known two-scroll (two-wing) butterfly chaotic attractor. Just after this, this system came as a prototype model for studying chaotic behaviour for quite a long time. During the past half-century, extensive studies have focused on chaos phenomena, and many fundamental characteristics of chaos have been identified.

On the other hand, in 1984, Chua proposed a new chaotic system, called a Chua circuit,[2] which is different from the Lorenz attractor from the viewpoint of smoothness of the nonlinear parts of the chaotic system. This system is also the pioneering work for a new research direction about new chaotic attractors.

Chaotic systems which have been proposed during the last four decades can be classified into two completely different classes: Lorenz-like chaotic systems and Chua-like chaotic systems. The nonlinear terms of the Chua-like systems, in comparison with the nonlinear terms of the Lorenz-like systems, usually include piecewise-linear continuous or discontinuous functions such as stair function, switching function, and hysteresis series function, which are not smooth functions.[3−5]

In Ref. [6], Lu *et al.* classified the three-dimensional smooth autonomous chaotic systems according to the number of the scrolls of the attractors generated from these system, i.e. systems generating a one-scroll attractor;[7−10] systems generating a two-scroll attractor;[11−14] systems generating a four-scroll attractor.[15,16] Later, in Ref. [17], a three-dimensional autonomous chaotic system was proposed which can generate three-scroll chaotic attractors. Recently, some 3D chaotic systems have been reported that can generate different multi-scroll chaotic attractors. In Refs. [18] and [19], Wang proposed 3D chaotic systems that can generate three- and four-scroll attractors. Also, Chen *et al.*[20] found another 3D chaotic system that can generate three-wing and four-wing attractors. In Ref. [21], Dadras *et al.* introduced a 3D chaotic system generating two-, three- and four-scroll chaotic attractors.

As explained above, most of the introduced chaotic systems were 3D autonomous systems. This might be due to the fact that the four-dimensional (4D) chaotic systems are more complex and chaos generation in 4D autonomous systems is more difficult than in 3D autonomous systems. Besides, generating

†Corresponding author. E-mail: momeni_h@modares.ac.ir

© 2010 Chinese Physical Society and IOP Publishing Ltd

different multi-scroll attractors from 4D chaotic systems is very difficult. In 2005,[22] Qi *et al.* proposed a 4D chaotic system. In 2006,[23] the same authors reported that the aforementioned system[22] could generate two coexisting single-wing attractors and two coexisting two-wing attractors by adding a constant control term. In 2007,[24] Liu *et al.* proposed a 4D chaotic system with a one-scroll attractor. In 2009,[25] Qi *et al.* added a simple state feedback term to the 4D system,[22] so it can generate only two- and four-scroll chaotic attractors.

In spite of the natural curiosity and extreme efforts made to generate a 3D and 4D autonomous system with different multi-scroll chaotic attractors, there have been reports on neither a 4D chaotic system nor a 3D chaotic system which can generate one-, two-, three- and four-scroll chaotic attractors by changing its parameters up to now.

In this paper, a novel four-dimensional autonomous chaotic system with five real equilibria is introduced and some basic dynamical behaviour of the new system is investigated. By varying the system coefficients, this new system can generate one-, two-, three- and four-scroll chaotic attractors. Interestingly, it is found that the new chaotic system can generate all the different multi-scroll attractors by changing only one single parameter while the other parameters are fixed. It ought to be stressed that this system exhibits all the attractors without adding any control term to its state equation. Numerical simulations are carried out in order to demonstrate the obtained analytical results. The interesting findings clearly show that this is a special strange new chaotic system which deserves further detailed investigation.

2. Novel chaotic attractor

Consider the following four-dimensional (4D) dynamic system with quadratic nonlinear terms:

$$\begin{cases} \dot{x} = ax - yz - w, \\ \dot{y} = xz - by + z, \\ \dot{z} = xy - cz + x, \\ \dot{w} = -w - dx, \end{cases} \tag{1}$$

where $x(t)$, $y(t)$, $z(t), w(t) \in R$ are the state variables, and a, b, $c \in R^+$ and $d \in R$ are constant parameters of the system.

2.1. Dissipativity and existence of the attractor

There are a few definitions of chaotic dynamics in the contemporary literature, but the common parts of all these definitions are the existence of local instability and exponential divergence of initially close trajectories. This can be shown by verifying the dissipativity of the system. The relationship between the dissipativity and the divergence of the vector field is

$$\begin{aligned} \frac{1}{V}\frac{\mathrm{d}V}{\mathrm{d}t} &= \operatorname{div} \boldsymbol{V} = \frac{\partial \dot{x}}{\partial x} + \frac{\partial \dot{y}}{\partial y} + \frac{\partial \dot{z}}{\partial z} + \frac{\partial \dot{w}}{\partial w} \\ &= a - b - c - 1 < 0. \end{aligned} \tag{2}$$

As the divergence of vector field (2) is negative, it can be concluded that system (1) is dissipative. It should be noticed that system (1) will always be dissipative if and only if $a < b + c + 1$ with an exponential rate

$$\frac{\mathrm{d}\boldsymbol{V}}{\mathrm{d}t} = \mathrm{e}^{a-b-c-1}. \tag{3}$$

Hence, volume element V_o is contracted by the flow into volume element $V_o\,\mathrm{e}^{(a-b-c-1)\,t}$ in time t. This means that each volume containing the system orbit shrinks to zero as $t \to \infty$ at exponential rate $(a - b - c - 1)$, which is independent of x, y, z, and w. Consequently, all system orbits will ultimately be confined to a specific subset of zero volume and the asymptotic motion settles onto an attractor. This suggests that the dynamics may tend to an attractor as $t \to \infty$.

2.2. Representation of equilibrium points

The spatial distribution and the local dynamical linearized characteristics of the equilibria greatly influence the dynamics of the system. The equilibrium points of system (1) can be easily found by solving the following algebraic equations simultaneously

$$\begin{cases} ax - yz - w = 0, \\ xz - by + z = 0, \\ xy - cz + x = 0, \\ -w - dx = 0. \end{cases} \tag{4}$$

Obviously, $O(0, 0, 0)$ is one equilibrium point. Furthermore, from Eq. (4), one has

$$w = -dx, \quad \text{and} \quad x = \frac{1}{a+d}yz. \tag{5}$$

Next, in order to solve Eq. (4), one can define the following new parameters:

$$\begin{aligned} &f = a + d, \quad \Delta = \sqrt{1 + 4fc}, \\ &\Gamma = \sqrt{f^2 + bf(-1 + \Delta)^2}, \\ &\Lambda = \sqrt{f^2 + bf(-1 - \Delta)^2}, \end{aligned} \tag{6}$$

and denote the five equilibrium points of system (1) respectively as

$$\begin{aligned} &O(0,0,0,0), \ E_1(x_1,y_1,z_1,w_1), \ E_2(x_2,y_2,z_2,w_2), \\ &E_3(x_3,y_3,z_3,w_3), \ \text{and} \ E_4(x_4,y_4,z_4,w_4), \end{aligned} \tag{7}$$

where

$$\begin{cases} O(0,0,0,0), \\ E_1\left(\dfrac{-f+\Gamma}{2f}, \dfrac{-1+\Delta}{2}, \dfrac{-f+\Gamma}{-1+\Delta}, \dfrac{d(f-\Gamma)}{2f}\right), \\ E_2\left(\dfrac{-f-\Gamma}{2f}, \dfrac{-1+\Delta}{2}, \dfrac{-f-\Gamma}{-1+\Delta}, \dfrac{d(f+\Gamma)}{2f}\right), \\ E_3\left(\dfrac{-f+\Lambda}{2f}, \dfrac{-1-\Delta}{2}, \dfrac{-f+\Lambda}{-1-\Delta}, \dfrac{d(f-\Lambda)}{2f}\right), \\ E_4\left(\dfrac{-f-\Lambda}{2f}, \dfrac{-1-\Delta}{2}, \dfrac{-f-\Lambda}{-1-\Delta}, \dfrac{d(f+\Lambda)}{2f}\right). \end{cases} \tag{8}$$

When $a = 7$, $b = 25$, $c = 11$, and $d = 0.5$, the five equilibria are

$$\begin{cases} O(0,\ 0,\ 0,\ 0), \\ E_1(15.2033,\ 8.5967,\ 13.2638,\ -7.6017), \\ E_2(-16.2033,\ 8.5967,\ -14.1362,\ 8.1017), \\ E_3(17.0282,\ -9.5967,\ -13.3079,\ -8.5141), \\ E_4(-18.0282,\ -9.5967,\ 14.0894,\ 9.0141). \end{cases} \tag{9}$$

Here, the stability of the zero equilibrium O is discussed. By linearizing system (1) at O, one obtains the Jaccobian

$$\begin{aligned} J_O &= \begin{bmatrix} a & -z & -y & -1 \\ z & -b & x+1 & 0 \\ y+1 & x & -c & 0 \\ -d & 0 & 0 & -1 \end{bmatrix} \\ &= \begin{bmatrix} 7 & 0 & 0 & -1 \\ 0 & -25 & 1 & 0 \\ 1 & 0 & -11 & 0 \\ -0.5 & 0 & 0 & -1 \end{bmatrix}. \end{aligned} \tag{10}$$

So, the eigenvalues of the linearized system are obtained as follows:

$$\begin{aligned} &|\lambda I - J_O| = 0 \Rightarrow \lambda_1 = -25, \quad \lambda_2 = -11, \\ &\lambda_3 = 7.062, \ \text{and} \ \lambda_4 = -1.062. \end{aligned} \tag{11}$$

Since λ_1, λ_3, $\lambda_4 < 0$, and $\lambda_2 > 0$, one can easily find that equilibrium O is unstable, i.e. the origin is an unstable saddle point for system (1).

The stability analysis of the nonzero equilibrium can be studied in a similar manner to that for equilibrium O. The numerical calculation results are shown in Table 1. It can be seen that system (1) has five equilibrium points which are all unstable saddle focus-nodes.

Table 1. Eigenvalues of the Jacobian matrix for all the equilibria.

λ	O	E_1	E_2	E_3	E_4
λ_1	–25	2.6989+14.5930i	2.5976+15.1452i	3.5795+14.8669i	3.5032+15.3752i
λ_2	–11	2.6989-14.5930i	2.5976–15.1452i	3.5795-14.8669i	3.5032-15.3752i
λ_3	7.06202	–34.39732667	–34.19472551	–36.15513636	–36.00273925
λ_4	–1.06202	–1.000419094	–1.000394367	–1.003937089	–1.003728086

3. Dynamical structure of the new chaotic attractors

System (1) is found to be chaotic over a wide range of parameters and exhibits abundant complex chaotic dynamical behaviours. Remarkably, this chaotic system can display one-, two-, three- and four-scroll attractors by varying only one single parameter while the others are fixed, which is a unique criterion for a four-dimensional chaotic system.

Remark 1 The numerical simulation is carried out by using the MATLAB program. The fourth order Runge–Kutta integration algorithm is performed to solve the differential equations. The initial condition is set to be $[10,\ 1,\ -10,\ 1]^{\mathrm{T}}$.

Remark 2 All the simulations are run with fixed parameters $a = 7$, $b = 25$, and $d = 0.5$ while parameter c varies.

3.1. Four-scroll chaotic attractor

The new chaotic system can display a four-scroll chaotic attractor if the parameter $c = 11$, which is depicted in Fig. 1. The four-wing chaotic attractor viewed in the x–y–z space is shown in Fig. 1(d), and the projections of phase portrait in x–y, y–z and z–ω planes are shown in Figs. 1(a), 1(b), and 1(c), respectively. As can be seen, the system generates a four-scroll chaotic attractor and the orbit is in chaos independent of the initial region. System (1) has five real equilibria which are shown in Eq. (9). The corresponding Lyapunov exponents are $l_1 = 2.468892$, $l_2 = 0$, $l_3 = -1.064744$, $l_4 = -30.803709$ (Table 2). The Lyapunov dimension (LD) of this system is

$$D_{\mathrm{L}} = j + \frac{1}{|l_{j+1}|}\sum_{i=1}^{j} l_i = 3 + \frac{l_1 + l_2 + l_3}{|l_4|} = 3 + \frac{2.468892 + 0 - 1.064744}{|-30.803709|} \approx 3.0456, \tag{12}$$

which means that the Lyapunov dimension of the four-scroll chaotic attractor is fractional. The Lyapunov dimension in Eq. (12) is calculated by the following approach: If there is no positive LE, then the LD is zero; if there are positive Lyapunov exponents, then LD is $D_L = j + \sum_{i=1}^{j} l_i/|l_{j+1}|$, where j is defined by the condition that $\sum_{i=1}^{j} l_i \geq 0$, and $\sum_{i=1}^{j+1} l_i \leq 0$.

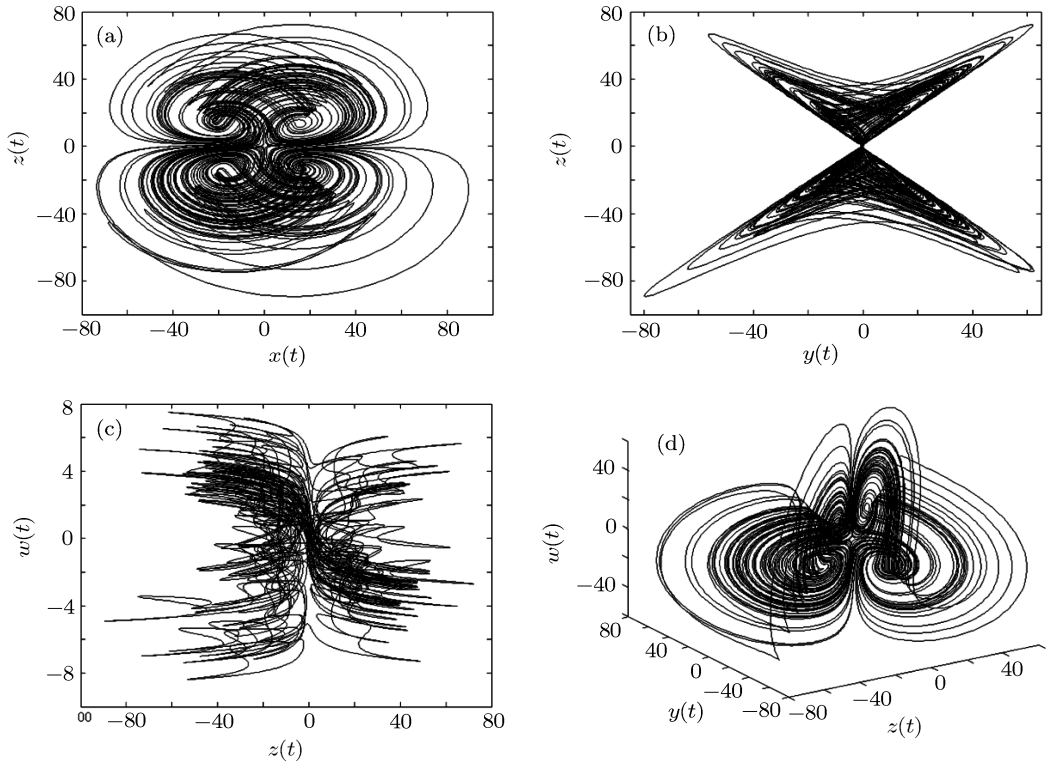


Fig. 1. Phase portraits of the four-scroll chaotic attractor for $a = 7$, $b = 25$, $c = 11$, and $d = 0.5$.

3.2. Three-scroll chaotic attractor

To generate a three-scroll chaotic attractor, we choose the varying parameter c to be 4.3, i.e. $c = 4.3$. In this case, again the system has five real equilibrium points. The Lyapunov exponents of the system in this case are $l_1 = 1.268248$, $l_2 = 0$, $l_3 = -1.042722$, $l_4 = -23.372221$ (Table 2). From Figs. 2(a)–2(d), one can clearly see that the four-dimensional quadratic autonomous chaotic system (1) can display an attractor with three scrolls.

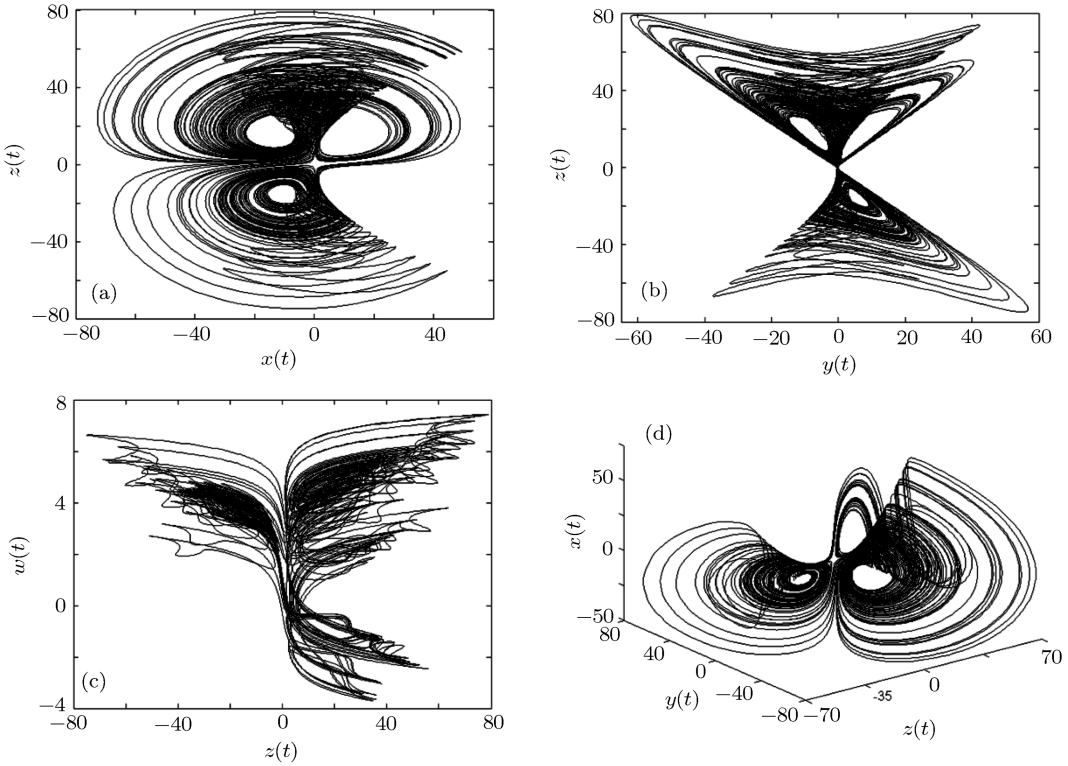


Fig. 2. Phase portraits of the three-scroll chaotic attractor for $a = 7$, $b = 25$, $c = 4.3$, and $d = 0.5$.

3.3. Two-scroll chaotic attractor

When $c = 20$, system (1) goes into another chaotic motion with Lyapunov exponents $l_1 = 0.899837$, $l_2 = 0$, $l_3 = -1.043168$, and $l_4 = -37.686280$ (Table 2). The phase portraits of system (1) are shown in Figs. 3(a)–3(d). It can be seen that system (1) can generate a two-scroll chaotic attractor.

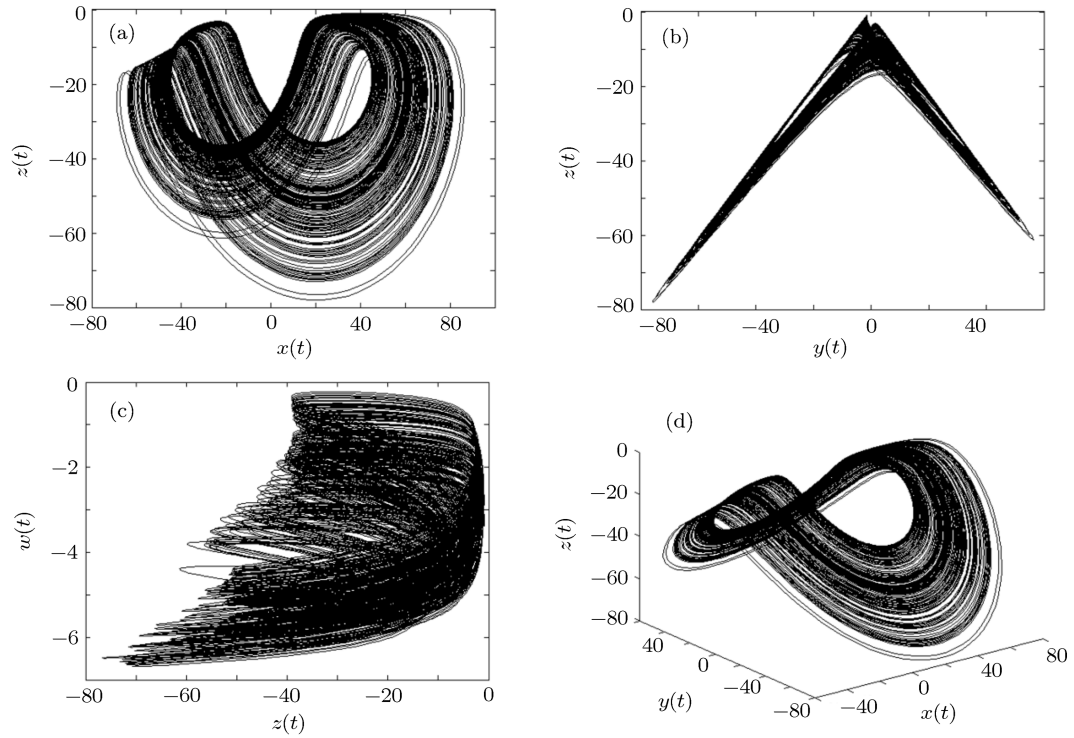


Fig. 3. Phase portraits of the two-scroll chaotic attractor for $a = 7$, $b = 25$, $c = 20$, $d = 0.5$.

3.4. One-scroll chaotic attractor

On further changing parameter c, system (1) can display a one-scroll attractor. Figures 4(a)–4(d) show the observation in different projective planes, in which parameter c is assumed to be 3.8. With this choice, the Lyapunov exponents of system (1) are $l_1 = 0.499404$, $l_2 = 0$, $l_3 = -1.017300$, and $l_4 = -22.163718$.

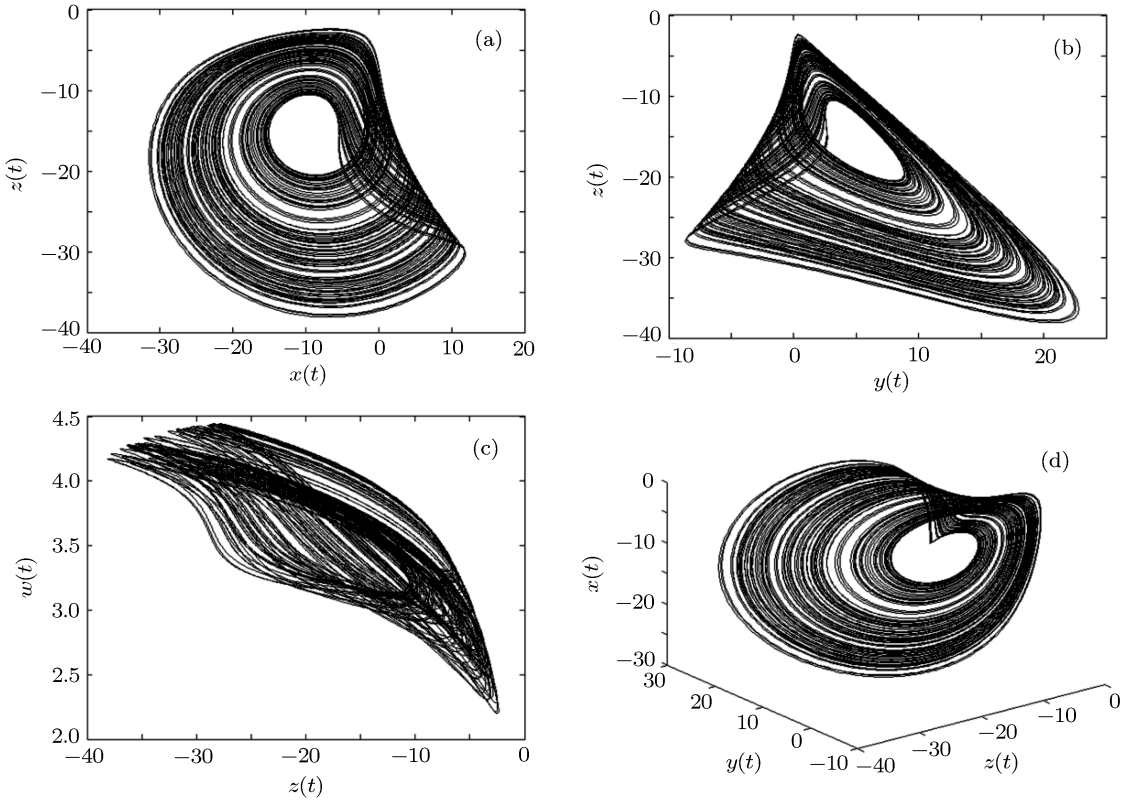


Fig. 4. Phase portraits of the one-scroll chaotic attractor for $a = 7$, $b = 25$, $c = 3.8$, and $d = 0.5$.

Figures 5(a)–5(d) illustrate the chaos trajectory evolutions of one-scroll, two-scroll, three-scroll and four-scroll attractors generated by new system (1) for different values of parameter c.

According to Figs. 1–5 and Table 2, it can be concluded that system (1) can display one-, two-, three-, and four-scroll chaotic attractors by varying only one single parameter. So, it is obvious that system (1) has more complex behaviours than all the 4D chaotic systems which we have known.

Table 2. Lyapunov exponents and dynamical behaviour for different values of parameter c.

c	l_1	l_2	l_3	l_4	dynamical behaviour
3.23	0.00	–0.131105	–1.074804	–20.938915	one-scroll periodic orbit
3.8	0.499404	0.00	–1.017300	–22.163718	one-scroll chaotic attractor
4.3	1.268248	0.00	–1.042722	–23.372221	three-scroll chaotic attractor
11	2.468892	0.00	–1.064744	–30.803709	four-scroll chaotic attractor
18.06	0.00	–0.122679	–1.064430	–35.182345	four-scroll periodic orbit
20	0.899837	0.00	–1.043168	–37.686280	two-scroll chaotic attractor
22.5	0.00	–0.746268	–1.008828	–39.187369	two-scroll periodic orbit

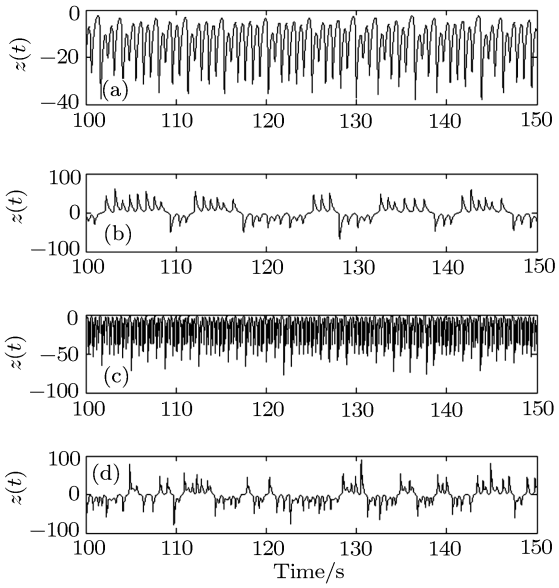


Fig. 5. Time responses of the third state of system (1) with $a = 7$, $b = 25$, $d = 0.5$: (a) $c = 3.8$, (b) $c = 4.3$, (c) $c = 20$, (d) $c = 11$.

4. Lyapunov exponent spectrum and bifurcation diagram

Bifurcation diagrams can be used to locate the transitions between periodic motion and chaotic motion. The bifurcation diagram of state x in a range of $c \in [2, 24]$ is shown in Fig. 6, and the corresponding spectra of Lyapunov exponents are depicted in Figs. 7(a) and 7(b). The system parameters are set to be $a = 7$, $b = 25$, $d = 0.5$ while parameter c is varied.

When $c < 3.43$, the maximum Lyapunov exponent is zero, implying that new system (1) is in a periodic mode; while for $c \in [3.43, 13.73]$, the maximum Lyapunov exponent $l_1 \in [0, 3]$ which indicates that system (1) is chaotic in the aforementioned range. In the window $c \in (13.73, 14.67)$, the maximum Lyapunov exponent equals zero, implying that the system has a periodic orbit. In the region $14.67 \leq c \leq 15.68$, the system is chaotic with a positive Lyapunov exponent, and the interval $c \in (15.68, 17.07]$ is a periodic subregion. Again, when $17.07 < c \leq 17.95$, the maximum Lyapunov exponent is positive and the system is in a chaotic mode. As $c \in (17.95, 18.25]$, system (1) exhibits periodic behaviour. From the spectrum of Lyapunov exponents of the system for $c \in (18.25, 20.33]$, shown in Fig. 7, one can clearly see that system (1) is chaotic except for a few tiny periodic windows. Finally, when $c > 20.33$, the maximum Lyapunov exponent almost equals zero and the bifurcation of x eventually changes into a periodic orbit. The whole evolution process can be clearly seen from the bifurcation diagram shown in Fig. 6, which illustrates the dynamics of state variables. Figure 8, from which the initial transients have been omitted for clarity, shows different periodic behaviours of the new chaotic system (1). Also, detailed evolutions among periodic orbits and chaos (different multi-scroll chaotic attractors) are shown in Table 2. Denoting by l_1, l_2, l_3, and l_4 the Lyapunov exponents of system (1) in Table 2, system (1) evolves into different modes in some typical different intervals of parameter c.

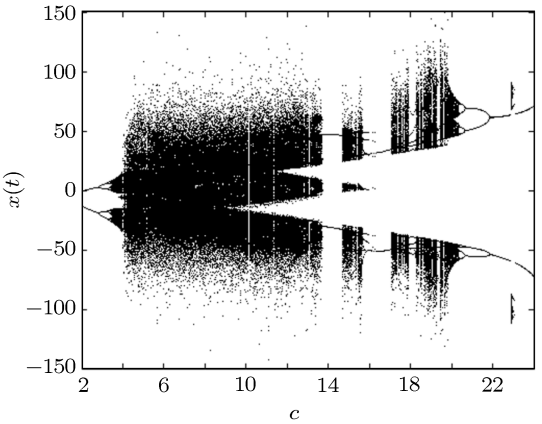


Fig. 6. Bifurcation diagram of the first state system (1) versus parameter c.

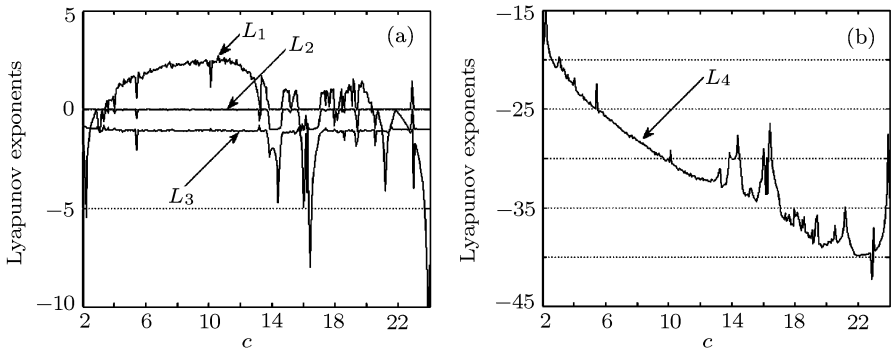


Fig. 7. Spectra of Lyapunov exponents of system (1) versus parameter c.

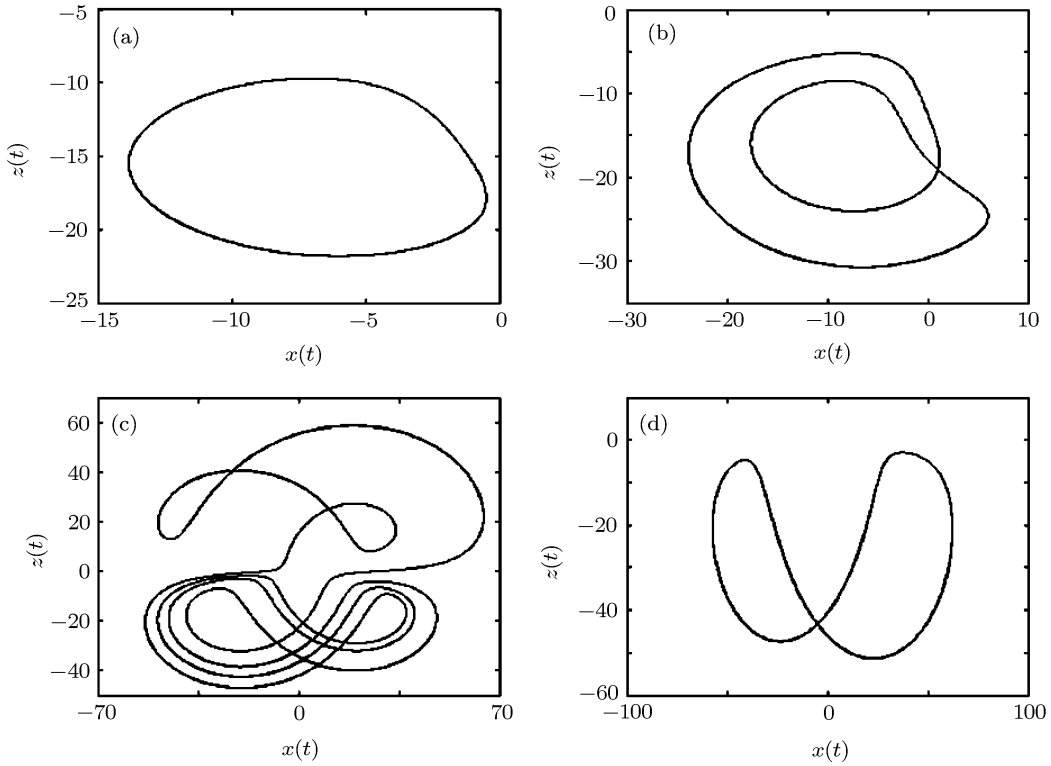


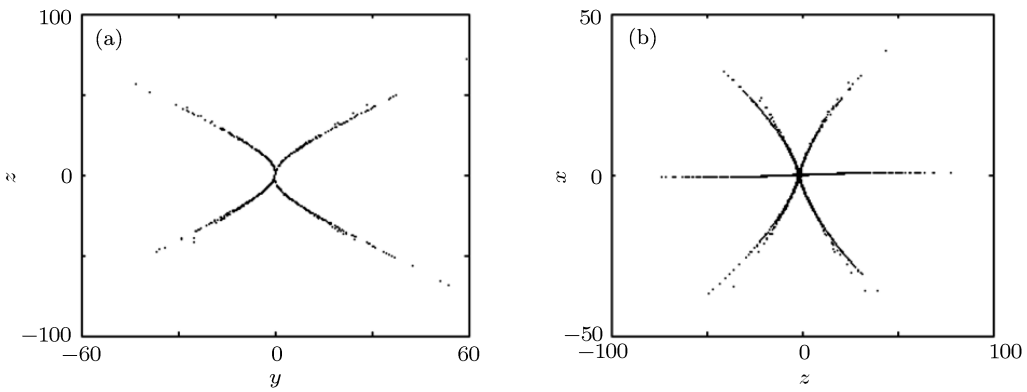
Fig. 8. Periodic phase portraits in the x–z plane, $a = 7$, $b = 25$, $d = 0.5$: (a) $c = 2.1$, (b) $c = 3.23$, (c) $c = 18.06$, (d) $c = 22.5$.

5. Poincaré mapping

As an important technique, a Poincaré map can reflect bifurcation and the folding properties of chaos. We take

$$\Sigma_1 = \{[x, y, z, w]^{\mathrm{T}} \in R^4 \big| \, x = 0\}, \quad \Sigma_2 = \{[x, y, z, w]^{\mathrm{T}} \in R^4 \big| \, y = 0\},$$
$$\Sigma_3 = \{[x, y, z, w]^{\mathrm{T}} \in R^4 \big| \, z = 2\}, \quad \Sigma_4 = \{[x, y, z, w]^{\mathrm{T}} \in R^4 \big| \, w - 2y = -1\}, \tag{13}$$

as cross sections and the system parameters are set to be $a = 7$, $b = 25$, $c = 11$, and $d = 0.5$. Figures 9(a), 9(b) 9(c) and 9(d) are projections of the Poincaré map in the y–z, z–x, x–w and x–z planes, respectively. From Figs. 9(a), 9(b) and 9(d), one can see that the Poincaré map here consists of several limbs with various bifurcations in different directions, which indicates that the system has extremely rich dynamics. Also, the Poincaré maps show that the branches are jointed and united as a single attractor. This proves the existence of the four-scroll chaotic attractor in Fig. 1.



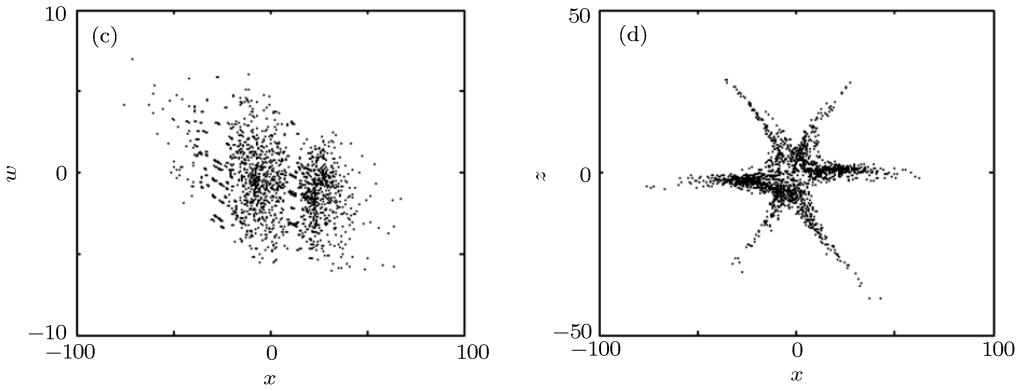


Fig. 9. Poincaré maps with system parameters $a = 7$, $b = 25$, $c = 11$, and $d = 0.5$ in different crossing sections: (a) $x = 0$, (b) $y = 0$, (c) $z = 2$, (d) w–$2y = -1$.

6. Conclusion

In this paper, we have illustrated the generating of one-, two-, three- and four-scroll attractors from a novel 4D autonomous chaotic system. This new system has complicated topological structures, and many other complex dynamics, over a wide range of parameters. The system possesses five equilibrium points. Basic properties of the new dynamical system are analysed by means of Lyapunov exponents, a Poincaré map and bifurcation diagrams. Stricter analysis of the complex characteristics of the new chaotic system is left for further studies.

References

[1] Lorenz E N 1963 *J. Atmos. Sci.* **20** 130

[2] Matsumoto T, Chua L O and Tanaks S 1984 *Phys. Rev.* A **30** 1155

[3] Baghious E and Jarry P 1993 *Int. J. Bifur. Chaos* **3** 201

[4] Elwakil A, Ozoguz S and Kennedy M 2002 *IEEE Trans. Circuits Syst.* I **49** 527

[5] Ozoguz S, Elwakil A and Kennedy M 2002 *Int. J. Bifur. Chaos* **12** 1627

[6] Lü J, Chen G and Cheng D 2004 *Int. J. Bifur. Chaos* **14** 1507

[7] Genesio R and Tesi A 1992 *Automatica* **28** 531

[8] Rössler O E 1976 *Phys. Lett.* A **57** 397

[9] Rössler O E 1976 *Ann. New York Acad. Sci.* **316** 376

[10] Sprott J C 1994 *Phys. Rev.* E **50** R647

[11] Chen G and Ueta T 1999 *Int. J. Bifur. Chaos* **9** 1465

[12] Lü J and Chen G 2002 *Int. J. Bifur. Chaos* **12** 659

[13] Liu C, Liu L, Liu T and Li P 2006 *Chaos, Solitons and Fractals* **28** 1196

[14] Shilnikov A L 1993 *Physica* D **62** 338

[15] Liu W B and Chen G 2003 *Int. J. Bifur. Chaos* **12** 261

[16] Qi G, Chen G, Wyk M A, Wyk B J and Zhang Y 2008 *Chaos, Solitons and Fractals* **38** 705

[17] Li D 2008 *Phys. Lett.* A **37** 387

[18] Wang L 2009 *Chaos* **19** 013107-1

[19] Wang L 2009 *Nonlinear Dynamics* **56** 453

[20] Chen Z, Yang Y and Yuan Z 2008 *Chaos, Solitons and Fractals* **38** 1187

[21] Dadras S and Momeni H R 2009 *Phys. Lett.* A **373** 3637

[22] Qi G, Du S, Chen G, Chen Z and Yuan Z 2005 *Chaos, Solitons and Fractals* **23** 1671

[23] Qi G, Chen G and Zhang Y 2006 *Phys. Lett.* A **352** 386

[24] Liu L, Liu C and Zhang Y B 2008 *J. Phys.: Conf. Ser.* **96** 012172

[25] Qi G, Wyk B J and Wyk M A 2009 *Chaos, Solitons and Fractals* **40** 2016